Neurotoxicology 69 (2018) 266–277

Contents lists available at ScienceDirect

Neurotoxicology

journal homepage: www.elsevier.com/locate/neuro

Full Length Article

Effects of environmental pollutants on calcium release and uptake by rat cortical microsomes

Hanna M. Dusza[a,b], Peter H. Cenijn[a], Jorke H. Kamstra[a,c], Remco H.S. Westerink[b], Pim E.G. Leonards[a], Timo Hamers[a,*]

[a] Vrije Universiteit Amsterdam, Dept. Environment & Health, The Netherlands
[b] Utrecht University, Institute for Risk Assessment Sciences, The Netherlands
[c] Norwegian University of Life Sciences, Dept. of Basic Science and Aquatic Medicine, CoE CERAD, Oslo, Norway

ARTICLE INFO

Keywords:
Ryanodine receptor
SERCA
IP_3 receptor
Environmental pollutants
Calcium homeostasis
Neurotoxicity
Microsomes

ABSTRACT

Dysregulation of neuronal intracellular Ca^{2+} homeostasis can play a crucial role in many neurotoxic effects, including impaired brain development and behavioral dysfunctions. This study examined 40 suspected neurotoxicants from different chemical classes for their capacity to alter Ca^{2+} release and uptake from rat cortical microsomes. First, ten suspected neurotoxicants have been tested using a well-established cuvette-based Ca^{2+} flux assay. Five out of ten compounds (TOCP, endosulfan, PCB-95, chlorpyrifos and BDE-49) showed a significant, concentration-dependent alteration of Ca^{2+} release and uptake in adult rat cortical microsomes. The original cuvette assay was downscaled and customized to a fast, higher throughput microplate method and the 40 suspected neurotoxicants were screened for their effects on intracellular Ca^{2+}homeostasis. In decreasing order of potency, the 15 test compounds that showed the strongest alteration of Ca^{2+} levels in adult rat microsomes were TOCP, endosulfan, BDE-49, 6-OH-BDE-47, PCB-95, permethrin, alpha-cypermethrin, chlorpyrifos, bioallethrin, cypermethrin, RDP, DEHP, DBP, BDE-47, and PFOS. Results from co-exposure experiments with selective inhibitors suggested that for some compounds Ca^{2+} releasing effects could be attributed to RyR activation (PFOS, DBP, and DEHP) or to SERCA inhibition (a potential novel mechanism of action for all four tested pyrethroid insecticides). The effects of the two most potent compounds, endosulfan and TOCP, were not blocked by any of the inhibitors tested, indicating other possible mechanism of action. For all other potent test compounds, a combined effect on RyR, IP_3R, and/or SERCA has been observed. PFOS and 6-OH-BDE-47 caused increased Ca^{2+} release from adult but not from neonatal rat brain microsomes, indicating age-dependent difference in susceptibility to these test compounds. The current study suggests that the neurotoxic potential of compounds belonging to different chemical classes could partly be attributed to the effects on intracellular Ca^{2+} release and uptake. Although further validation is required, the downscaled method developed in this study presents technical advance that could be used for the future screening of suspected intracellular Ca^{2+} disruptors.

Abbreviations: 6OH-BDE-47, 6-hydroxy-2,2',4,4'-tetrabromodiphenylether; BDE-47, 2,2',4,4'-tetrabromodiphenylether; BDE-49, 2,2',4,5'-tetrabromodiphenylether; DBP, dibutylphthalate; DEHP, diethylhexyl phthtalate; DHBP, 1,1'-diheptyl-4,4'-bipyridinium dibromide; DMSO, dimethylsulfoxide; DOPO, 9,10-dihydro-9-oxa-10-phosphaphenanthrene 10-oxide; ER, endoplasmic reticulum; IP3R, inositol 1,4,5-triphosphate receptor; MEHP, monoethylhexyl phthalate; PBDE, polybrominated diphenyl ether; PBDPP, 1,3-Phenylene bis(diphenyl phosphate); PCB, polychlorinated biphenyl; PCB-95, 2,2',3,5',6-pentachlorobiphenyl; PFAS, polyfluorinated alkylated substance; PFOA, perfluorinated octanoic acid; PFOS, perfluorooctane sulfonate; R3, three months old female rat; R6, six months old female rat; RDP, resorcinol bis(diphenylphosphate), also known as PBDPP; RN, neonatal, (3–4 days old) unsexed rat pups; RyR, ryanodine receptor; SERCA, sarco/endoplasmic reticulum Ca2+ ATPase; TDCPP, tris(1,3-dichloroisopropyl)phosphate; TOCP, tri-o-cresyl phosphate; TP1, 2-[3-Bromo-1-(3-chloro-2-pyridinyl)-1H-pyrazol-5-yl]-6-chloro-3,8 dimethyl-4(3 H)-quinazolinone, transformation product of chlorantraniliprole in basic water; TP2, 2-[3-Bromo-1-(3-hydroxy-2-pyridinyl)-1H-pyrazol-5-yl]-6-chloro-3,8-dimethyl-4(3 H)-quinazolinone, transformation product of chlorantraniliprole after photolysis; VGCC, voltage-gated calcium channel; VGClC, voltage-gated chloride channel; VGSC, voltage-gated sodium channel

* Corresponding author at: Vrije Universiteit Amsterdam, Department Environment & Health, De Boelelaan 1085, 1081 HV Amsterdam, The Netherlands.
E-mail address: timo.hamers@vu.nl (T. Hamers).

https://doi.org/10.1016/j.neuro.2018.07.015
Received 11 December 2017; Received in revised form 26 June 2018; Accepted 25 July 2018
Available online 26 July 2018

1. Introduction

Environmental pollutants are increasingly recognised for their ability to alter development and function of the nervous system (Grandjean and Landrigan, 2006, 2014). The prenatal period of brain development is particularly vulnerable to chemical exposure because of temporal and regional emergence of critical developmental processes that form the basis for cognitive and behavioral function (Paterson et al., 2006; Rice and Barone, 2000). Several different classes of chemicals have been identified as developmental neurotoxicants. For example, *in utero* exposure to methylmercury and lead causes severe neurobehavioral effects including cerebral palsy and mental retardation in children (Hu et al., 2006; Myers and Davidson, 1998). More recently, prenatal exposure to polychlorinated biphenyls (PCBs) and polybrominated diphenyl ethers (PBDEs), has been associated with decrements in neonatal reflexes, motor activity, cognitive functions and hearing impairments in studies of both humans and animals (Darras, 2008; Herbstman et al., 2010; Jolous-Jamshidi et al., 2010; Kenet et al., 2007; Roze et al., 2009). Additionally, exposure to the organophosphate pesticide chlorpyrifos has been linked to delayed neurodevelopment, increased occurrence of attention deficit hyperactivity disorder (ADHD) and lower IQ scores in children (Rauh et al., 2011, 2006), whereas exposure to organochlorine pesticides and phthalates has been associated with increased risk of autism spectrum disorders (Lyall et al., 2017; Testa et al., 2012). Despite the many associations, the modes of action by which environmental pollutants can induce various neurotoxic effects are still largely unknown.

Ca^{2+} signaling, a spatial and temporal fluctuation of intracellular Ca^{2+} levels, plays a major role in regulating a vast range of developmental processes, including gene expression and cell proliferation (Verkhratsky and Parpura, 2014). Ca^{2+} homeostasis is of particular importance in neuronal cells since transient increments in neuronal cytoplasmic Ca^{2+} level regulate many neuronal processes, including differentiation and synaptogenesis, synaptic plasticity and neurotransmission (Berridge et al., 2000; Rizzuto, 2001). Thus, the disruption of neuronal Ca^{2+} dynamics could be one of the important mechanisms responsible for impaired brain development and function observed following chemical exposure (Pessah et al., 2010).

Intracellular Ca^{2+} homeostasis is regulated by a combination of Ca^{2+} entry and release from the extracellular space and intracellular Ca^{2+} stores. Ca^{2+} uptake and release from intracellular Ca^{2+} stores is mediated by a system of different Ca^{2+} channels and pumps present in the plasma membrane and endoplasmic reticulum (ER). Ryanodine receptors (RyRs) and inositol 1,4,5-trisphosphate receptors (IP_3Rs) regulate the stimuli-evoked Ca^{2+} release from the ER into the cytosol, whereas the active sarco/endoplasmic reticulum Ca^{2+} ATPase (SERCA) transporter restores the intracellular Ca^{2+} levels through active transport of excess Ca^{2+} back into ER (Berridge et al., 2000). A considerable amount of literature highlighting the importance of SERCA, RyR and IP_3R in intracellular Ca^{2+} signaling provides evidence that disruption of these mechanisms could trigger neurotoxicity (Bodalia et al., 2013; Gleichmann and Mattson, 2011; Marambaud et al., 2009).

Previously, Wong et al. (1997) demonstrated that ortho-substituted PCBs induce Ca^{2+} release from rat brain microsomes by selectively activating the RyRs. Later studies showed that perfluorooctane sulphonate (PFOS) and perfluorooctanoate (PFOA) can elevate Ca^{2+} levels through RyR and IP_3R-mediated mechanism in cultured hippocampal neurons (Liu et al., 2011). Additionally, different PBDE congeners, *e.g.* BDE-47, BDE-99 and 6-OH-BDE-47, were also shown to inhibit release and uptake of Ca^{2+} into the microsomes isolated from different regions of rat brain (Coburn et al., 2008; Kodavanti and Ward, 2005). A more recent study by Gassmann et al. (2014) on human neural progenitor cells indicated that modulation of Ca^{2+} homeostasis by BDE-47 and 6-OH-BDE-47 is caused by RyR-independent mechanisms. However, for many known and newly emerging neurotoxicants effects on intracellular Ca^{2+} homeostasis are still poorly investigated. Considering the wealth of environmental pollutants and the potential central role of disruption of Ca^{2+} homeostasis in cellular neurotoxicity (*e.g.* Westerink, 2014), sensitive and robust high throughput *in vitro* assays are required for a comprehensive understanding of the mechanisms of neurotoxicity and accurate hazard characterization.

More than twenty years ago, Wong and Pessah (1996) developed a RyR-based method to investigate neurotoxic effects of PCBs on intracellular Ca^{2+} signaling. While this assay was demonstrated to be useful in predicting risk and biological activity of suspected neurotoxicants, it is also labor-intensive. The aim of the present study was to adapt the original cuvette-based assay to a higher throughput format in order to screen a battery of environmentally relevant chemicals (pesticides, flame retardants, plasticizers, perfluorinated compounds and metals) for their potency to alter Ca^{2+} release and uptake from rat cortical microsomes (ER membrane). The potential mechanisms of action (*i.e.* interaction with Ca^{2+} sensitive release channel complexes (RyR and IP_3R) or interaction with ATP-dependent SERCA) as well as the effects of the test compounds at different stages of mammalian brain development were also investigated.

2. Material and methods

2.1. Compounds

A list of 40 suspected neurotoxic compounds from 13 chemical classes was compiled (Table 1). Chlorpyrifos-oxon and dianizon-o-analog were purchased from Accu-Standard (New Haven, CT). Tri-o-cresyl phosphate (TOCP), perfluorooctanoic acid (PFOA) and DMSO were obtained from Acros (Geel, Belgium), 9,10-dihydro-9-oxa-10-phosphaphenanthrene 10-oxide (DOPO) from Krems Chemie (Krems an der Donau, Austria), and resorcinol bis(diphenylphosphate) (RDP, also known as PBDPP) from ICL-IP (Terneuzen, The Netherlands). Brominated flame retardant 2,2′,4,4′-tetra-bromodiphenyl ether (BDE-47) and its hydroxylated metabolite 6-OH-BDE-47 were generously provided by Åke Bergman (Stockholm University). All other test compounds (Table 1) as well as 4-bromo-calcium ionophore A23187, fluo-3, 1,1′-diheptyl-4,4′-bipyridinium dibromide (DHBP), heparin, and thapsigargin were purchased from Sigma (Sigma-Aldrich, Zwijndrecht, The Netherlands). All chemicals were purchased at the highest commercially available purity.

2.2. Stock solutions and reagents

Test compounds were dissolved in DMSO to a final stock concentration of 10 mM. Lower-concentration stocks were prepared by serial dilution in DMSO. Stock solution of DHBP and thapsigargin were prepared by dissolving the compounds in DMSO to 100 mM and 5 mM, respectively. Stock solution of heparin was prepared by dissolving in demi water to a final concentration of 100 mg/ml. Fluo-3 was dissolved in DMSO to a final stock concentration of 1 mM. All stock solutions were prepared in glass vials with polypropylene screw caps and stored at 20 °C.

All reagents used for preparation of assay buffer and ATP regeneration system were purchased from Sigma (Sigma-Aldrich, Zwijndrecht, The Netherlands). The assay buffer consisted of 40 mM KCl, 62.5 mM KH_2PO_4, 1 mM NaN_3, 10 µM K-EGTA, 8 mM MOPS and was kept at 4 °C for one month at maximum. To prepare the ATP regeneration system consisting of 11.83 mM MgATP, 60 mM phosphocreatine and 0.1 kU/ml creatine phosphokinase in assay buffer, first a 10-fold stock of MgATP (118.3 mM) and phosphocreatine (600 mM) was prepared in assay buffer and stored in 100 µl aliquots at -20 °C. Before use, 29 µl creatine phosphokinase (3.5 kU/ml in 0.25 M Gly/Gly buffer; pH = 7.4) was added to the aliquot followed by addition of 871 µl assay buffer to a final volume of 1.0 ml containing the ATP regeneration system. A 1.5 mM stock solution of $CaCl_2$ was prepared in demi water to load the microsomes with Ca^{2+}. Stock solutions of fluo-3,

Table 1
Net Ca^{2+} release (pmol/(mg*min) and uptake (1/min) from cortical microsomes of 6 month (R6) and 3 months old (R3) female rats and neonatal rat pups (RN) exposed to 10 µM of the test compounds, as measured in the microplate assay. Data represents the average value (SD) of n = 2 measurements, unless indicated differently. The 15 highest Ca^{2+} release rates for the R6 microsomes are shaded in grey.

Chemical class	Compound	CAS number	Type[a]	Net Ca^{2+} release (pmol/(mg*min))			Net Ca^{2+} uptake (1/min)		
				R6	R3	RN	R6	R3	RN
Organophosphate insecticide	Chlorpyrifos	2921-88-2	P	162 (15)	311 (17)	61 (13)	0.08 (0.04)	0.08 (0.01)	0.10 (0.00)
	Chlorpyrifos-oxon	5598-15-2	M	19 (5)	-	-	0.09 (0.03)	-	-
	Parathion	56-38-2	P	70 (2)	7 (8)	-24 (11)	0.11 (0.03)	0.09 (0.01)	0.14 (0.00)
	Paraoxon-ethyl	311-45-5	M	51 (12)	-	-	0.12 (0.01)	-	-
	Paraoxon-methyl	950-35-6	M	49 (7)	-	-	0.14 (0.00)	-	-
	Dimethoate	60-51-5	P	76 (18)	-	-	0.13 (0.00)	-	-
	Omethoate	1113-02-6	M	62 (7)	-	-	0.13 (0.01)	-	-
	Diazinon	333-41-5	P	68 (22)	-	-	0.13 (0.01)	-	-
	Diazinon-O-analog	962-58-3	M	42 (6)	-	-	0.13 (0.01)	-	-
	Dichlorvos	62-73-7	P	65 (16)	-	-	0.14 (0.00)	-	-
Carbamate insecticide	Aldicarb	116-06-3	P	28 (9)	-	-	0.13 (0.03)	-	-
	Carbaryl	63-25-2	P	80 (10)	-	-	0.13 (0.01)	-	-
	Pirimicarb	23103-98-2	P	41 (8)		-	0.12 (0.02)	-	-
	Methomyl	16752-77-5	P	56 (2)	-	-	0.13 (0.00)	-	-
Pyrethroid insecticide	Permethrin[b]	52645-53-1	P	176 (17)	320 (98)	93 (7)	0.09 (0.00)	0.08 (0.00)	0.09 (0.00)
	Bioallethrin	584-79-2	P	145 (8)	203 (92)	73 (13)	0.11 (0.01)	0.08 (0.00)	0.10 (0.00)
	Alpha-cypermethrin	67375-30-8	P	169 (2)	318 (28)	75 (15)	0.10 (0.01)	0.09 (0.02)	0.10 (0.00)
	Cypermethrin[b]	52315-07-8	P	141 (1)	297 (56)	54 (18)	0.09 (0.00)	0.09 (0.00)	0.10 (0.00)
Diamide insecticide	Chlorantraniliprole	500008-45-7	P	46 (11)	-	-	0.10 (0.00)	-	-
	TP1[c]	-	TP	86 (4)	-	-	0.09 (0.00)	-	-
	TP2[c]	-	TP	54 (2)	-	-	0.10 (0.00)	-	-
	Flubendiamide	272451-65-7	P	41 (21)	-	-	0.11 (0.00)	-	-
Organochlorine insecticide	Dicofol	115-32-2	P	71 (19)	-	-	0.15 (0.01)	-	-
	Endosulfan[d]	115-29-7	P	237 (33)[e]	418 (61)	63 (15)[e]	0.08 (0.01)[e]	0.07 (0.00)	0.10 (0.01)[e]
Neonicotinoid insectide	Imidacloprid	138261-41-3	P	50 (3)	-	-	0.14 (0.02)	-	-
Bipyridyl herbicide	Paraquat	75365-73-0	P	18 (8)	-	-	0.19 (0.01)	-	-
Organophosphate flame retardant	TDCPP	13674-87-8	P	39 (3)	-	-	0.16 (0.01)	-	-
	TOCP	78-30-8	P	252 (20)	516 (73)	110 (11)	0.09 (0.01)	0.08 (0.01)	0.09 (0.00)
	RDP	57583-54-7	P	126 (1)	231 (78)	83 (1)	0.12 (0.01)	0.10 (0.00)	0.12 (0.02)
	DOPO	35948-25-5	P	-25 (10)	-	-	0.17 (0.02)	-	-
Brominated flame retardant	BDE-47	5436-43-1	P	98 (11)	143 (29)	54 (57)	0.11 (0.01)	0.09 (0.00)	0.13 (0.02)
	6-OH-BDE-47	79755-43-4	M	215 (15)	405 (17)	7 (3)	0.10 (0.00)	0.07 (0.00)	0.12 (0.01)
	BDE-49	243982-82-3	P	220 (26)	427 (59)	120 (23)	0.09 (0.01)	0.07 (0.00)	0.09 (0.01)
Phthalate	DBP	84-74-2	P	102 (13)	165 (74)	31 (7)	0.07 (0.02)	0.11 (0.00)	0.12 (0.00)
	DEHP	117-81-7	P	104 (24)	196 (70)	34 (15)	0.07 (0.01)	0.10 (0.00)	0.09 (0.01)
	MEHP	4376-20-9	P	-20 (33)	-	-	0.10 (0.00)	-	-
Perfluorinated compound	PFOA	335-67-1	P	-59 (20)	-	-	0.11 (0.01)	-	-
	PFOS	2795-39-3	P	82 (30)	387 (29)	-1 (24)	0.08 (0.01)	0.10 (0.00)	0.12 (0.01)
Organochlorine	PCB-95	38379-99-6	P	210 (6)	397 (12)	67 (1)	0.06 (0.00)	0.06 (0.01)	0.10 (0.00)
Organometal	Methylmercury	115-09-3	P	66 (21)	-	-	0.09 (0.01)	-	-
Control	DMSO	67-68-5	SC	0 (21)[e]	0 (54)	0 (14)[e]	0.14 (0.04)[e]	0.11 (0.01)	0.14 (0.03)[e]

[a]Type of compound refers to P: parent compound; M: metabolite; TP: transformation product; SC: solvent control.
[b]mixture of cis and trans isomers.
[c]TP1 and TP2 are both transformation products of chloranthroniliprole: TP1 in basic water and TP2 after photolysis (Lavtizar et al., 2014).
[d]2:1 mixture of alpha and beta stereoisomers.
[e]Since no differences were observed between microplates, duplicates for DMSO and endosulfan were pooled from different experiments, *i.e.* n = 6 for R6 and n = 4 for RN.

microsomes and ATP regeneration system were kept on ice during the experiments.

2.3. Membrane preparation

Adult brain microsomal fractions were obtained from six (R6) and three (R3) months old female Wistar rats (240–340 g) after euthanization with CO_2, whereas neonatal brain microsomal fractions (RN) were obtained from 3 to 4 days old, unsexed rat pups after decapitation. Cerebral cortex was immediately dissected, snap-frozen with liquid nitrogen and stored at −80 °C. Microsomal vesicles were prepared by modification of the methods described previously by Zimányi and Pessah (1991) and Rengifo et al. (2007). Briefly, tissue from cerebral cortex was defrosted on ice and homogenized with 10-fold (w/v) ice-cold homogenization buffer consisting of 250 mM sucrose, 5 mM HEPES, 1 mM EGTA, 1 mM DTT, protease inhibitor cocktail (Sigma P8340; 100x diluted) with pH 7.4 (adjusted with KOH). Homogenization was done with a glass/teflon Potter Elvehjem homogenizer with transformator speed set at 40 rpm. Homogenate was centrifuged at 1000 g and 4 °C for 10 min. The resulting supernatant was collected, the pellet resuspended in a half of the initial volume of homogenization buffer and centrifuged at 8000 *g* for 10 min and 4 °C. The pellet was discarded and the supernatant centrifuged at 100 000 *g* and 4 °C for 75 min. Protein concentration of the final pellet was determined by Bradford protein assay (Bio-Rad, The Netherlands). The final pellet was resuspended in homogenization buffer without EGTA at a protein concentration of 10 mg/ml and stored at −80 °C until use.

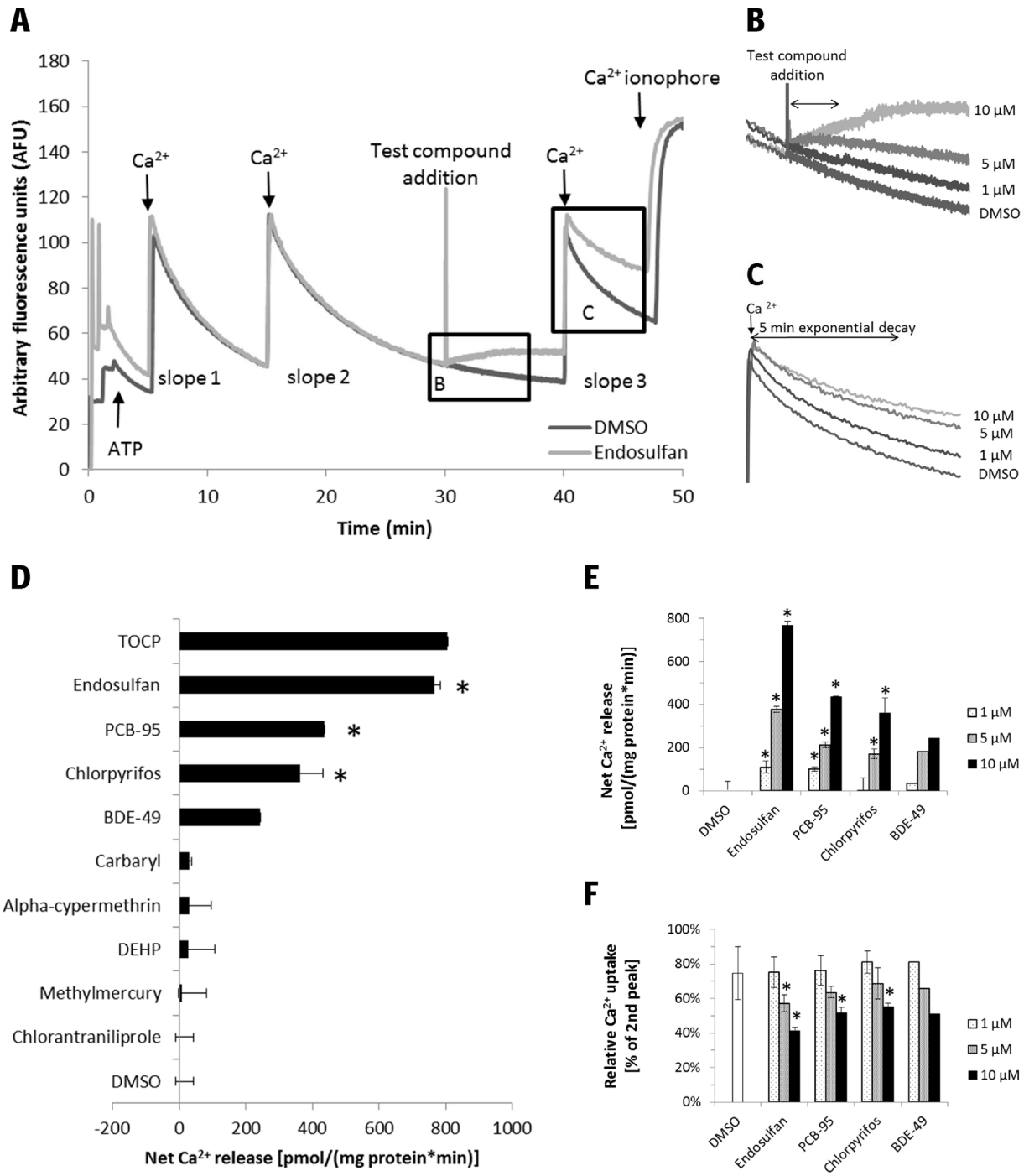

Fig. 1. Alteration of net Ca^{2+} release and uptake in cuvettes by cerebral cortex microsomes obtained from 6 months old female rat (R6). A) Typical traces of fluorescence following Ca^{2+} loadings (slopes 1, 2, and 3), demonstrating the effect of 10 µM endosulfan on Ca^{2+} release and Ca^{2+} uptake as compared to DMSO control. B) Detail trace of net Ca^{2+} release and C) Reduction in net Ca^{2+} uptake induced by endosulfan showing a concentration-dependent effect. D) Net Ca^{2+} releases slopes induced by test compounds at 10 µM concentration. E) Concentration-dependent Ca^{2+} release for four positive controls. F) Concentration-dependent decrease of Ca^{2+} uptake for four positive compounds, expressed as the ratio between first order Ca^{2+} uptake rates of slope 3 and slope 2. Error bars represent standard deviation between independent experiments (n = 2; except for TOCP and BDE-49 (n = 1)). Asterisks (*) indicate significant difference to DMSO control ($p < 0.05$).

2.4. Ca^{2+} flux measurement

Measurements of the intracellular Ca^{2+} concentration, reflecting the net balance between cellular Ca^{2+} influx, buffering and extrusion, typically rely on single cell Ca^{2+} imaging with cell permeable Ca^{2+} indicator dyes. In the current experiments, however, microsomes are studied directly to reveal the role of intracellular Ca^{2+} stores and Ca^{2+} is measured in the extra-microsomal fraction using a membrane-impermeable Ca^{2+} indicator fluo-3. The Ca^{2+} flux measurement was based on the method previously described by Wong et al. (1997) and Pessah et al. (2006). A sub-set of test compounds, including PCB-95 as a positive control, was tested as in the original papers using glass cuvette (Fig. 1D). After successful set-up of the cuvette method, the full list of test compounds was tested in a novel down-scaled, higher throughput

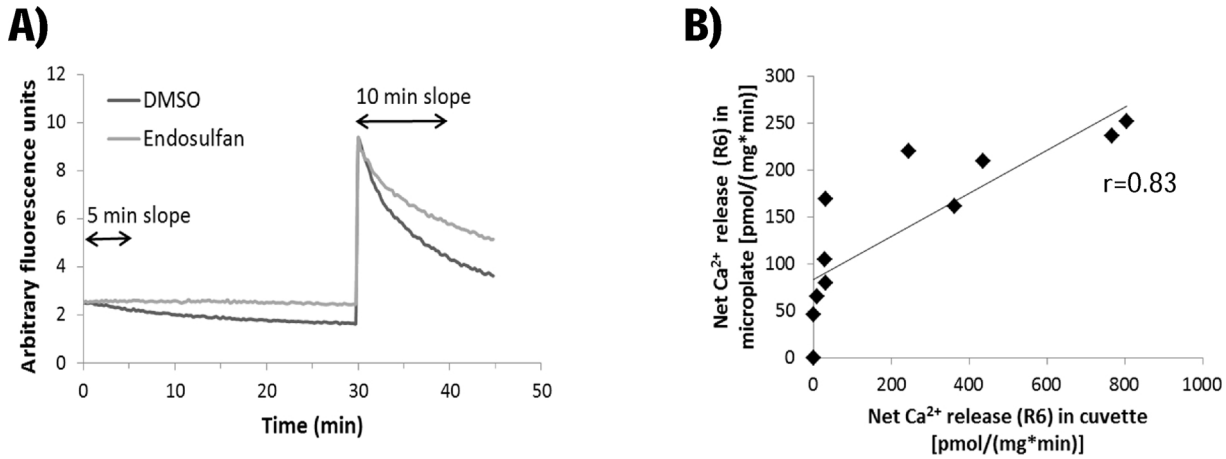

Fig. 2. Alteration of net Ca^{2+} release and uptake in microplates by cerebral cortex microsomes obtained from 6 months old female rat (R6). A) Typical traces of fluorescence, demonstrating the effect of 10 μM endosulfan on Ca^{2+} release and Ca^{2+} uptake as compared to DMSO control. The time frame shown corresponds to the time frame 30–45 min in Fig. 1A, *i.e.* end of slope 2 after test compound addition followed by the third Ca^{2+} spike (slope 3). B) Significant correlation between cuvette and microplate measurements of net Ca^{2+} release rates for 10 test compounds and a DMSO control.

screening method developed for the purpose of the present study.

2.4.1. Cuvette method

All measurements were performed in a temperature-controlled glass cuvette at 37 °C, with constant stirring. To each cuvette, 200 μl of ATP regeneration system, 1.2 μl of fluo-3 (final concentration 0.5 μM), and 80 μl (R6, final concentration 0.333 mg/ml) or 35 μl (R3, final concentration 0.146 mg/ml) microsomal protein was added to assay buffer (2.4 ml final volume). The protein concentration for R3 microsomes was adjusted in order to achieve the same basal Ca^{2+} uptake activity as seen with R6 microsomes. The net Ca^{2+} flux kinetics across the microsomes was recorded by measuring the fluorescence intensity of extra-microsomal free Ca^{2+} levels using the membrane impermeable Ca^{2+} indicator fluo-3 and a Cary Eclipse Fluorescence Spectrophotometer (Kinetic Software Version 1.1(133)), excitation and emission wavelengths set at 500 and 530 nm, respectively). Microsomal vesicles were loaded with Ca^{2+} by two additions of 12 μl of 1.5 mM $CaCl_2$ (2 × 18 nmol, final concentration 7.5 μM). After the signal of Fluo-3 returned to the baseline level (due to SERCA pumping extra-microsomal Ca^{2+} into the microsomes), microsomes were exposed to the test compound by addition of 2.4 μl of a 10 mM stock concentration in DMSO (final concentration 10 μM) and extra-microsomal Ca^{2+} level was further monitored (Fig. 1A and B). Four test compounds, *i.e.* endosulfan, PCB-95, chlorpyrifos and BDE-49 were additionally tested in 1 and 5 μM concentrations to reveal concentration-dependence. All experiments were performed at final DMSO concentration of 0.1%, except for BDE-49 (0.4% DMSO). DMSO solvent controls were included on each experimental day. Uptake of Ca^{2+} into the exposed microsomes was determined by loading the exposed microsomes with another 18 nmol $CaCl_2$ and measuring the decrease in extra-microsomal Ca^{2+} concentration (Fig. 1A and C). Ca^{2+} ionophore 4-bromo A23187 was used at the end of each measurement to release remaining accumulated Ca^{2+} from the microsomes.

2.4.2. Microplate method

Briefly, the amount of microsomes needed for each microplate assay was calculated and then pre-incubated in one big batch with final protein concentration of 0.333 mg/ml for R6 or RN and 0.146 mg/ml for R3. Microsomes were pre-incubated for 5 min in UV protected, polypropylene tubes with assay buffer containing ATP regeneration system and 0.5 μM fluo-3. Incubation was performed at 37 °C with constant stirring using an orbital shaker (VWR, Amsterdam, The Netherlands). The pre-incubated microsomes were then loaded under continuous stirring with two spikes of $CaCl_2$ (each contributing 7.5 μM to the final Ca^{2+} concentration), with 10 and 15 min of loading time, respectively. While microsomes were loaded with Ca^{2+} in the tubes, each well of a black non-binding, polypropylene, 96-wells flat-bottom microplate (Greiner, Germany) was filled with 2.4 μl of test compound (1 mM dissolved in DMSO). After the 30 min loading phase, 240 μl of Ca^{2+}-loaded microsomes suspended in assay buffer was transfered to each well of the 96-wells plate using an automatic pipette, yielding final concentrations of 10 μM for the test compounds in 1% DMSO. Reagents in the well were mixed by 10 s intensive shaking of the plate before each measurement. The ability of compounds to mobilize the accumulated Ca^{2+} from the vesicles was measured in the absence and in the presence of RyR-inhibitor DHBP (100 μM), IP_3R-inhibitor heparin (100 μg/ml), or SERCA-inhibitor thapsigargin (5 μM). Inhibitors were added to Ca^{2+}-loaded microsomal suspension in assay buffer 2 min before transfer to the plate. The Ca^{2+} flux kinetics were measured in a Varioskan Flash multimode reader (Thermo Scientific, Finland) with Skanit software 2.4.5 (Thermo Scientific, Finland) at a constant temperature of 37 °C. Fluorescence (λ_{ex} = 485 nm; λ_{em} = 525 nm) was followed in time for each well by 120 readings (200 ms) with 15 s interval in a kinetic loop. To allow this interval between readings, only half of the 96-wells plate was typically used in a single experiment. The effect of test compounds on the Ca^{2+} uptake into the exposed microsomes was determined by re-loading the exposed vesicles with a 1.8 nmol $CaCl_2$ spike per well and measuring the decrease in extra-microsomal Ca^{2+} concentration.

2.5. Data analysis

To allow comparison between different cuvettes, fluorescence measurements in the cuvette method were normalized for the increase in fluorescence caused by the second spike of Ca^{2+} in the loading phase. No such normalization was required for the microplate method, because all wells received an aliquot of the same large batch of Ca^{2+} loaded microsomes. The initial rates of Ca^{2+} release induced by the test compounds were obtained by linear regression analysis between 20–140 s (cuvette, Fig. 1B) or 20–300 s (microplate reader, Fig. 2A) of data measured after the start of exposure to the test compound. The rates of Ca^{2+} uptake in exposed microsomes were calculated by fitting a single exponential decay function to the Ca^{2+} measurements of the first 5 min (cuvette, Fig. 1C) or 10 min (microplate reader, Fig. 2A) after addition of an additional (third) Ca^{2+} spike. For the cuvette experiments, differences between independent treatments and DMSO controls were tested by one-way ANOVA with Dunnett's post-hoc test ($p < 0.05$). For the microplate experiments, differences between plates

were tested by two-way ANOVA with treatment (endosulfan and DMSO) and plate number as independent variables ($p < 0.05$). To determine expected positive correlation between results from cuvette and microplate experiments and between results from cortical microsomes of different age groups, and expected negative correlation between results from Ca^{2+} release and Ca^{2+} uptake measurements, Pearson's correlation coefficient was calculated and tested for significance ($p < 0.05$) by a one-sided t-test.

3. Results

3.1. Alteration of net Ca^{2+} release and uptake - cuvette measurements

A typical trace of extra-microsomal Ca^{2+} measured in the cuvette method is shown in Fig. 1A. Transport of Ca^{2+} into the microsomes (visible as a decline in the extra-microsomal Ca^{2+} concentration) was observed after ATP addition, confirming that Ca^{2+} uptake by the microsomal membrane was ATP-dependent (Wong et al., 1997). Two spikes of Ca^{2+} were taken up by the microsomes during the loading phase (Fig. 1A, slope 1 and 2). During exposure to 10 μM endosulfan, an increase in extra-microsomal Ca^{2+} was observed as compared to DMSO control. Ten minutes after compound exposure, microsomes were spiked with Ca^{2+} for the third time. The rate of Ca^{2+} uptake in the microsomes exposed to endosulfan was lower than with DMSO control (Fig. 1A, slope 3). Finally, accumulated Ca^{2+} could be released from the microsomes by the addition of the Ca^{2+} ionophore 4-bromo A23187.

Ca^{2+} release was quantified as the slope of the net Ca^{2+} release in the first two minutes after test compound addition (Fig. 1B). Five out of ten compounds representing different chemical classes induced net Ca^{2+} release from adult microsomes at 10 μM concentration as compared to DMSO control (Fig. 1D). TOCP and endosulfan demonstrated higher Ca^{2+} release from the microsomes than the positive control PCB-95. To test if these effects were concentration-dependent, microsomes were exposed to four positive compounds with different potencies, *i.e.* endosulfan, PCB-95, chlorpyrifos and BDE-49 in 1–10 μM range. All four compounds showed strong concentration-dependent effects (Fig. 1D and E), whereas none of the studied compounds significantly interfered with the dye fluo-3 (data not shown).

Ca^{2+} uptake was quantified by fitting a single exponential decay function to the Ca^{2+} measurements of the first 5 min after test compound addition (Fig. 1C). In the DMSO control trace, Ca^{2+} uptake slopes decreased in time with slope 3 < slope 2 < slope 1 (Fig. 1A). To determine if Ca^{2+} uptake rates were affected by the test compounds, the first-order Ca^{2+} uptake rate of slope 3 was expressed as a percentage of the first-order Ca^{2+} uptake rate of slope 2. For the four chosen positive controls, the rate of the net Ca^{2+} uptake into the microsomes decreased in a concentration-dependent manner as compared to DMSO control (Fig. 1F).

3.2. Microplate measurements

Although effective and robust, the cuvette method is inefficient considering the amount of material and time needed for each measurement. Alternatively, kinetic measurements in a microplate set-up are known to be challenging (Heusinkveld and Westerink, 2011). For instance, it is practically impossible to follow the Ca^{2+} loading phase in each separate well online, because this requires manual synchronization between addition of the Ca^{2+} spikes, addition of the test compounds, and measurement of the fluorescence, which would make the method prone to operator errors. We therefore customized and downscaled the existing cuvette-based Ca^{2+} release assay to a higher throughput version in 96-wells microplates, by adding the test compounds (dissolved in DMSO) to the plate in advance. In parallel, microsomes were preloaded with Ca^{2+} in a single, large-volume batch, of which aliquot volumes were subsequently dispensed in each well. Ca^{2+} release was quantified as the slope of the net Ca^{2+} release in the first five min after test compound addition (Fig. 2A), whereas Ca^{2+} uptake was quantified by fitting a single exponential decay function to the Ca^{2+} measurements of the first 10 min after Ca^{2+} spike addition (Fig. 2A). After pre-testing this method with reference compounds PCB-95 and endosulfan, all 40 suspected neurotoxicants were screened in duplicates for their potency to alter Ca^{2+} release and uptake from rat cortical microsomes obtained from adult female rats (R6) (Table 1). Three separate microplates were used to test all 40 compounds. In all three microplate experiments DMSO and endosulfan were tested as solvent control and positive control, respectively.

Similar to the cuvette measurements, exposure to endosulfan caused a significantly increased Ca^{2+} release from the Ca^{2+}-loaded microsomes compared to the DMSO solvent control and a significantly decreased microsomal Ca^{2+} uptake after addition of an additional Ca^{2+} spike (Fig. 2A). No difference in Ca^{2+} release or uptake was observed between separate microplate experiments and also no interaction effect was observed between exposure (*i.e.* DMSO or endosulfan) and experiments (*i.e.* different microplates). These results indicate that the microplate method is robust, and that results from different microplate experiments can be mutually compared if the same batch of microsomes is used.

The microplate screening of all 40 test compounds revealed other compounds being capable of causing microsomal Ca^{2+} release. The most potent compounds (in order of decreasing potency) were TOCP, endosulfan, BDE-49, 6-OH-BDE-47, PCB-95, permethrin, alpha-cypermethrin, chlorpyrifos, bioallethrin, cypermethrin, RDP, DEHP, DBP, BDE-47, and PFOS (Table 1). Ca^{2+} release rates for 10 compounds tested in the cuvette (Fig. 1D) were compared to Ca^{2+} release rates observed for these compounds in the microplate method. For those compounds, significant correlation was observed between the two methods ($r = 0.83$, Fig. 2B).

3.3. Ca^{2+} release and uptake in cortical microsomes at different stages of brain development

Since Ca^{2+} homeostasis plays a crucial role during brain development, additional microplate measurements of microsomal Ca^{2+} release and uptake were performed with microsomes obtained at different stages of brain development *i.e.*, from 3 months old rats (R3) and neonatal pups (RN). Sixteen compounds were tested, *i.e.* the 15 compounds with highest Ca^{2+} releasing rates from R6 microsomes in the microplate method (shaded grey in Table 1), extended with parathion as a representative compound with poor Ca^{2+} releasing properties. Most of the 15 potent compounds that showed effects on Ca^{2+} release in R6 microsomes also showed effects on Ca^{2+} release in R3 and RN microsomes (Table 1). The Ca^{2+} release rates observed for the R3 microsomes were almost two times higher than those observed for the R6 microsomes. Nevertheless, a significant, high correlation was found between Ca^{2+} release rates from R6 and R3 as measured in the microliter plate ($r = 0.87$; Fig. 3A). Two out of 16 compounds did not obey to this significant correlation ($r = 0.87$): exposure to PFOS caused a higher Ca^{2+} release rate by R3 microsomes than expected based on results with R6 microsomes, whereas the opposite effect was observed for parathion exposure (Fig. 3A). These data suggest that the Ca^{2+} releasing potency of compounds might be age dependent, possibly due to the temporal differential expression of different transporter isoforms (see Section 4.2). In general, Ca^{2+} release rates by RN microsomes were lower than observed for R3 or R6. RN microsomes showed better correlation with R6 (Fig. 3C) than R3 (Fig. 3E) microsomes, but both (significant) correlations were lower than between R6 and R3 microsomes (Fig. 3A). Most obvious differences were observed for PFOS and 6-OH-BDE-47. Both compounds showed high Ca^{2+} release rates by R6 and R3 microsomes, whereas no effect was observed for RN microsomes (Table 1).

The majority of the 15 compounds that showed effects on Ca^{2+}

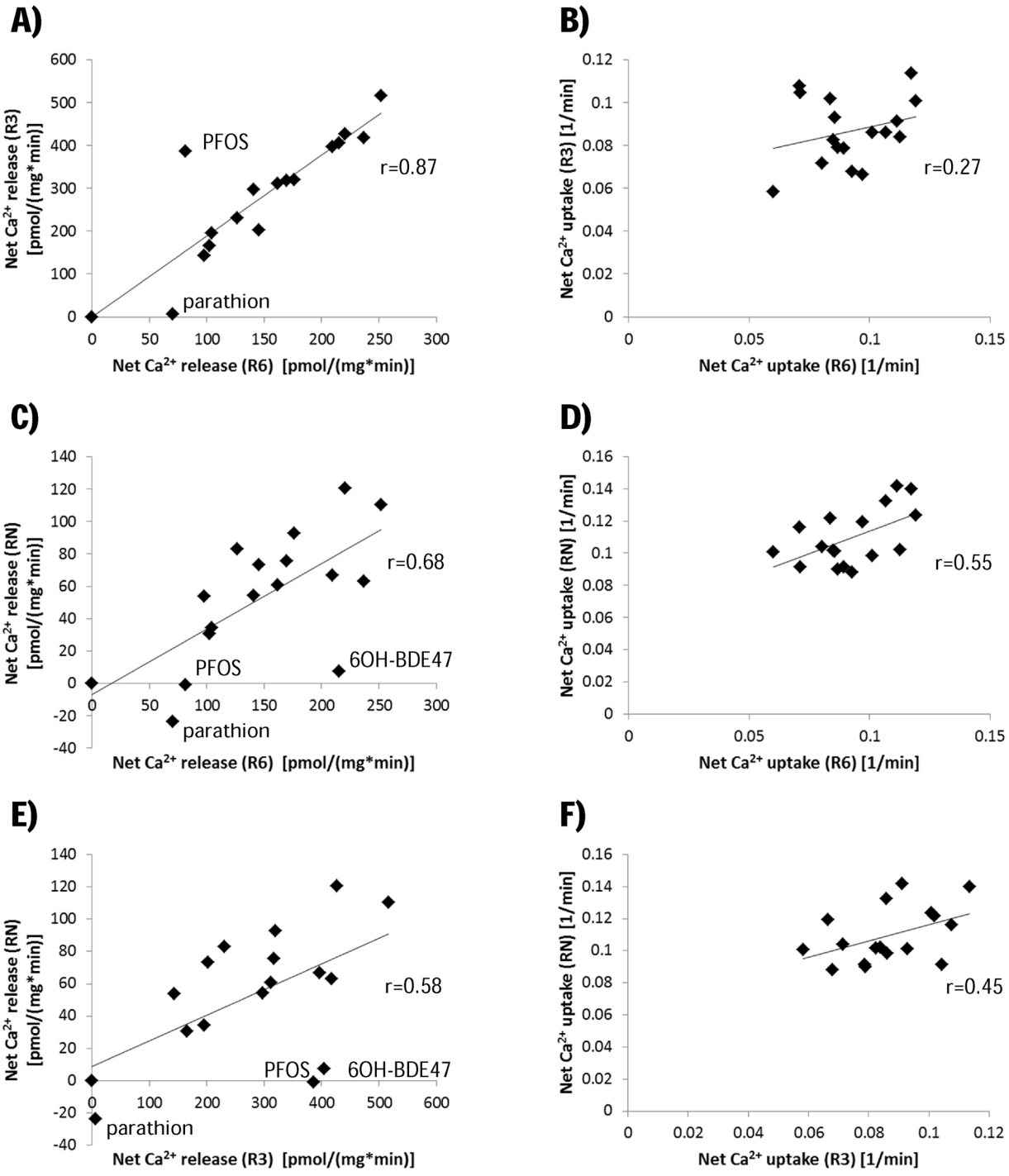

Fig. 3. Comparison of net Ca^{2+} release rates (left) and net Ca^{2+} uptake rates (right) as determined in the microplate method for microsomes from rats with different ages, *i.e.* 6-months (R6), 3-months (R3) or neonatal (RN) exposed to 16 different test compounds and a DMSO control. Correlation between R6 and R3 microsomes for A) Ca^{2+} release and B) Ca^{2+} uptake; Correlation between R6 and RN microsomes for C) Ca^{2+} release and D) Ca^{2+} uptake D); Correlation between R3 and RN microsomes for E) Ca^{2+} release and F) Ca^{2+} uptake. All correlations were statistically significant ($p < 0.05$), except for B (*i.e.* Ca^{2+} uptake by R6 and R3 microsomes).

release also showed effects on the Ca^{2+} uptake rates (Table 1). Whereas the effects of different test compounds on Ca^{2+} release rates differed by two orders of magnitude, effects on Ca^{2+} uptake rates were much less pronounced, irrespective of the age of the donor animals (Table 1). Correlations between Ca^{2+} uptake rates determined for different age classes were relatively low and in some cases non-significant (Fig. 3B, D, F), most likely due to the lack of distinctiveness in Ca^{2+} uptake rates between the different exposures. Consequently, no compounds could be distinguished that cause age-specific changes in Ca^{2+} uptake rates.

To test if the Ca^{2+} release rates observed for R3 microsomes in the microplate could also be replicated in the original cuvette method, the ten most potent compounds that were newly identified in the microplate as Ca^{2+} releasing were also tested in the cuvette (Fig. 4A). Remarkably, three out of the four pyrethroid insecticides causing Ca^{2+} release from R3 microsomes in the microplate method did not show any effect on Ca^{2+} release in the cuvette. Consequently, the correlation between Ca^{2+} release rate in the cuvette and microplate methods was relatively low for R3 microsomes, but still significant ($r = 0.53$;

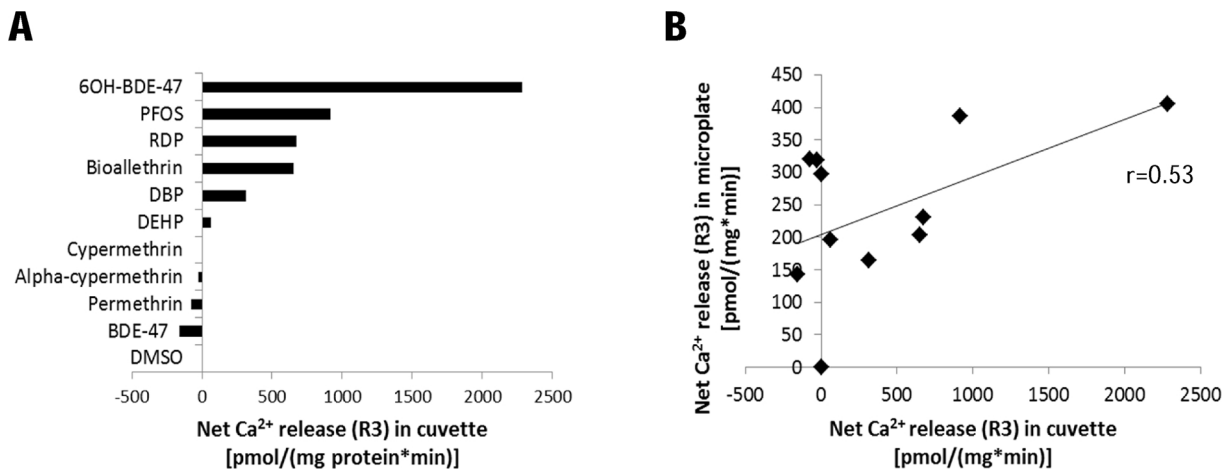

Fig. 4. Net Ca^{2+} release by cerebral cortex microsomes from 3 months old female rat (R3) exposed to 10 μM concentrations of test compounds. A) Results from the cuvette method; B) Correlation between net Ca^{2+} release rates determined by the cuvette method and the microplate method.

Fig. 4B).

3.4. Inhibitor experiments

Following compound exposures, Ca^{2+} uptake rates were negatively correlated with Ca^{2+} release rates for the different age classes, ranging from r = −0.56 for R6 to r = −0.76 for RN microsomes (Fig. S1). This negative correlation was to be expected, because changes in extra-microsomal Ca^{2+} concentration measured in the assay are the net result of increased Ca^{2+} release and decreased Ca^{2+} uptake. In other words, compounds opening Ca^{2+} channels RyR and IP_3R do not only cause an increase in Ca^{2+} release, but also contribute to a net decrease in Ca^{2+} uptake. The other way around, compounds inhibiting SERCA do not only cause a decrease in Ca^{2+} uptake, but are also responsible for a lack of compensation of Ca^{2+} release by RyR and IP_3R.

To further study the mechanism by which the test compounds affect Ca^{2+} release and uptake, microsomes were simultaneously exposed to test compounds and inhibitors of RyR, IP_3R, or SERCA (Fig. 5). Co-exposure to RyR inhibitor DHBP most obviously reduced the Ca^{2+} releasing effect of PFOS (by 84%), DBP (by 76%), and DEHP (by 71%), indicating that these compounds cause Ca^{2+} release mainly through RyR activation (Fig. 5A). For some compounds, *i.e.* PCB-95, chlorpyrifos, BDE-47, and 6-OH-BDE-47, Ca^{2+} release rates could possibly be attributed to a combined activation of RyR and IP_3R, given that ≥40% of the effects have been reduced after co-exposure to DHBP and to IP_3R inhibitor heparin (Fig. 5A and B). Co-exposure to SERCA inhibitor thapsigargin reduced the Ca^{2+} releasing effect of chlorpyrifos by 60% and BDE-49 by 55%, and - more specifically - of all pyrethroid insecticides tested, *i.e.* permethrin by 77%, bioallethrin by 56%, alpha-cypermethrin by 91% and cypermethrin by 91% (Fig. 5C). For chlorpyrifos, BDE-49 and bioallethrin the inhibition of Ca^{2+} release by thapsigargin strongly deviated between the replicates and the result for these compounds should be interpreted with caution. Nevertheless, the almost complete reduction of pyrethroid induced Ca^{2+} release by thapsigargin indicates the inhibition of the neuronal endoplasmic reticulum Ca^{2+} ATPase pump as a potential novel mechanism of action for this class of insecticides.

Interestingly, increased microsomal Ca^{2+} release rates were found for PFOS and 6-OH-BDE-47 when co-exposed to thapsigargin. This finding is to be expected for compounds that alter Ca^{2+} efflux channels, since SERCA pump inhibition disables the mechanism that pumps Ca^{2+} ions back into the ER vesicles, thereby enhancing the effect of compounds that cause an opening of the Ca^{2+} efflux channels *i.e.*, RyR (PFOS) or IP_3R (6-OH-BDE-47) (Fig. 5C). Finally, none of the three inhibitors had a distinct effect on the net Ca^{2+} release induced by the most potent compounds endosulfan and TOCP.

4. Discussion

4.1. Alteration of Ca^{2+} release and re-uptake in cortical microsomes

Using a novel microplate screening method, this study demonstrates that a range of environmental pollutants belonging to different chemical classes can alter Ca^{2+} release/uptake in microsomes from rat cerebral cortex by inhibition of RyR, IP3R and/or SERCA mediated mechanism.

4.1.1. PCB-95, PBDEs and perfluorinated compounds

It is well-known that ortho-substituted PCBs increase the intracellular Ca^{2+} concentration in numerous cell types, including cerebellar granule neurons (Llansola et al., 2010; Tan et al., 2004) and rat PC12 cells (Langeveld et al., 2012; Wong et al., 2001). Wong et al. (1997) previously demonstrated that PCB-95 mobilizes Ca^{2+} from neuronal microsomes in a concentration-dependent manner, which is in line with our results obtained from both cuvette and microplate reader measurements. Wong et al. (1997) also suggested that PCB-95 has a specific RyR activating mode of action, which we confirmed by demonstrating inhibition of Ca^{2+} release in the presence of the selective RyR channel blocker DHBP.

PBDEs and ortho-substituted PCBs share common molecular and cellular mechanisms (Westerink, 2014) by which they may interfere with neurodevelopmental processes. Similar to PCBs, PBDEs have previously been shown to affect Ca^{2+} homeostasis in microsomes isolated from adult rat frontal cortex, cerebellum, hippocampus and hypothalamus (Coburn et al., 2008; Kodavanti and Ward, 2005). In the present study all three PBDE compounds tested (*i.e.* BDE-47, BDE-49 and 6-OH-BDE-47) showed a significant increase in Ca^{2+} release in cortical microsomes of adult rats. In an earlier study, Kim et al. (2011) indicated that PBDEs induce Ca^{2+} release in neuronal cells by RyR mediated mechanism. The authors suggested that PBDEs with two ortho-bromine substituents and lacking at least one para-bromine substituent (*e.g.*, BDE-49) activate RyR1 and RyR2 with greater potency than corresponding congeners with two para-bromine substitutions (*e.g.*, BDE-47). These findings seem to be consistent with our results in which BDE-49 had twofold higher potency to induce Ca^{2+} release from adult rat microsomes than its congener BDE-47. Moreover, 6-OH-BDE-47 induced Ca^{2+} release following activation of protein lipase C and IP_3R in primary fetal human neural progenitor cells, which appeared to be independent of RyR (Gassmann et al., 2014). These results correspond with our observations (Fig. 5B), where the IP_3R channel blocker

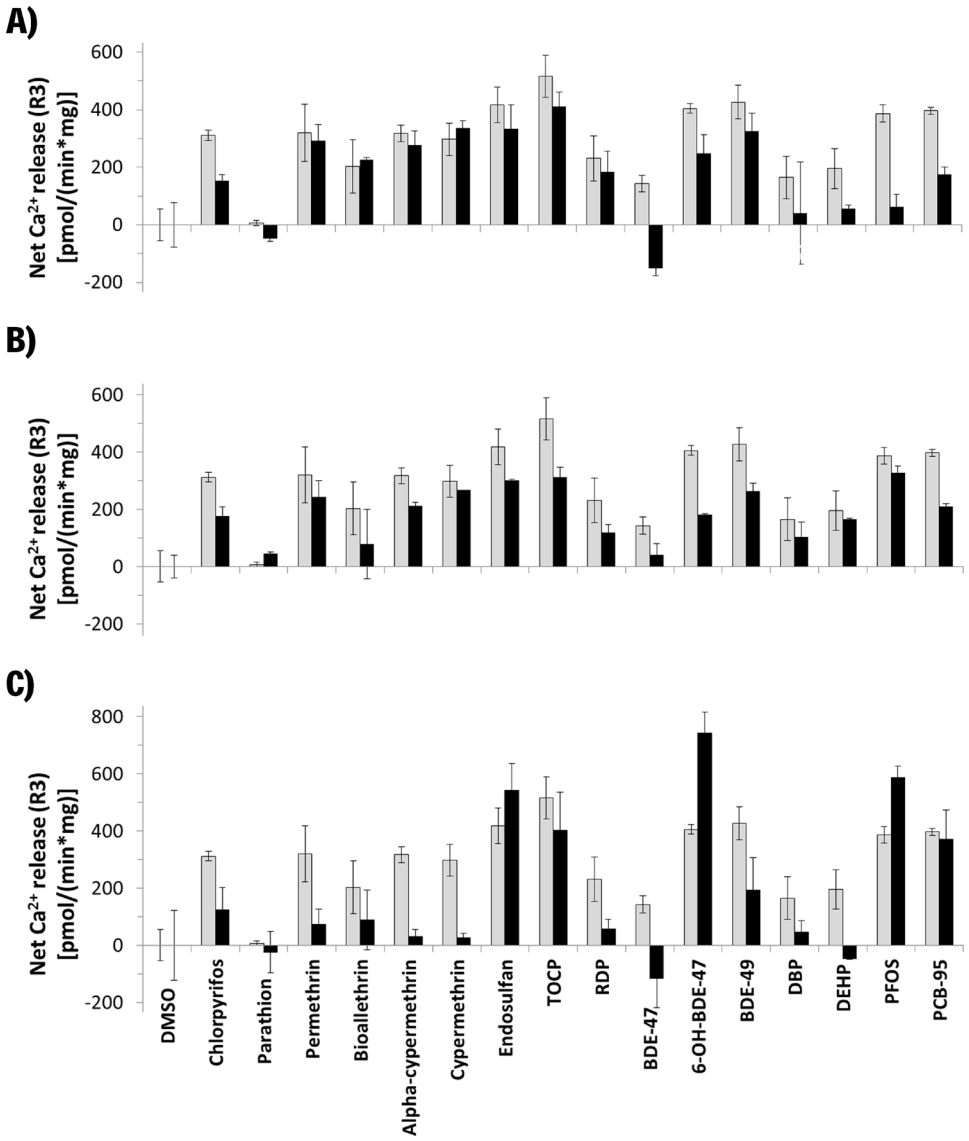

Fig. 5. Ca^{2+} release rates determined for microsomes from 3 months old female rats (R3) exposed to 10 μM test compound concentrations in the microplate. Microsomes were co-exposed to test compounds without inhibitor (grey bars) and inhibitors (black bars) of A) RyR (100 μM DHBP), B) IP_3R (100 μg/ml heparin), or C) SERCA (5 μM thapsigargin). Compound-specific Ca^{2+} release rates [pmol/(mg*min)] were normalized for their respective control exposures to DMSO. Error bars represent standard deviation of duplicate measurements within a single plate experiment (n = 1).

heparin inhibited more than 65% of the initial Ca^{2+} release induced by 6-OH-BDE-47.

Effects of perfluorinated alkylated substances (PFASs) on intracellular Ca^{2+} homeostasis in neuronal cells are hardly studied. In our study, sulfonated PFOS caused increased microsomal Ca^{2+} release, which was almost completely blocked by RyR channel blocker DHBP (Fig. 5A), whereas carboxylated PFOA was completely inactive (Table 1). These results corroborate with a study by Liu et al. (2011) who found larger increases in cytoplasmic Ca^{2+} levels in cultured hippocampal neurons exposed to PFOS than to PFOA. Based on co-exposure experiments with two specific antagonists of the intracellular ion channels, the authors speculated that the observed increased of cytoplasmic Ca^{2+} levels could be mediated by both IP_3R and RyR ion channels. For PFOS, the present study provides further evidence of RyR specific mobilization of intracellular Ca^{2+} stores.

PCBs, PBDEs and PFASs have previously been shown to exert diverse cellular effects, ranging from neuronal apoptosis (Howard et al., 2003; Wang et al., 2015), alteration of dendritic growth and morphogenesis (Chen et al., 2017; Wayman et al., 2012) and synaptic plasticity (Gilbert, 2000; Kim and Pessah, 2011) to behavioral deficits in animals and human (Herbstman et al., 2010; Kenet et al., 2007; Roze et al., 2009). Such effects can at least partially be attributed to disruption of Ca^{2+} signaling through RyR and/or IP_3-mediated mechanism (Pessah et al., 2010; Rizzuto, 2001), highlighting the importance of dysregulation of Ca^{2+} homeostasis in (human) neurodevelopmental disorders.

4.1.2. Pyrethroids

Most of the available literature link the neurotoxic effects of pyrethroids to their ability to alter voltage-gated sodium channels (VGSCs), which are crucial for neuronal excitability (for an extensive review see Soderlund (2012)). Additional reports indicate that pyrethroids can also inhibit voltage-gated calcium channels (VGCCs; *e.g.* Hildebrand et al., 2004; Meijer et al., 2014). However, little data exist on the effects of pyrethroids on intracellular Ca^{2+} channels and pumps. All four pyrethroids tested in our study (permethrin, cypermethrin, alpha-cypermethrin and bioallethrin) showed alteration of Ca^{2+} homeostasis in adult microsomes. The effect of pyrethroids on microsomal Ca^{2+} release was inhibited completely (alpha-cypermethrin and cypermethrin)

or partially (permethrin and bioallethrin) by the highly selective SERCA blocker thapsigargin (Michelangeli and East, 2011), suggesting high affinity of pyrethroid compounds towards the SERCA pump. To our knowledge the effect of pyrethroids on neuronal ER SERCA pump has never been reported in the literature before. Because the cortical microsomes used in our study originate primarily from intracellular endoplasmic reticulum, it is unlikely that the microsomes contained other functional ion pump and channels originating from the plasma membrane, thereby excluding possible interference of *e.g.*, VGSCs or VGCCs. Our results thus indicate a potential novel mechanism of action for this class of insecticides that hypothetically could account for some unexplained Ca^{2+} dependent effects observed in the literature, *e.g.* the increased Ca^{2+} levels observed by Cao et al. (2011) in neocortical neurons.

4.1.3. Phthalates and other test compounds

While very little is known about phthalates' potency towards neuronal intracellular targets such as Ca^{2+} channels and pumps, however DBP and DEHP have previously been shown to increase cytosolic Ca^{2+} levels in RBL-2H3 mast cells (Nakamura et al., 2002) and rat PC12 cells (Tully et al., 2000). In our study DBP and DEHP, but not its primary metabolite MEHP, induced Ca^{2+} release in microsomal vesicles with ~70% of the effect blocked by DHBP, indicating their RyR mediated mechanism of action. These data point to the potential importance of intracellular stores in phthalate mediated neurotoxicity that could serve as a basis for further investigation.

The increase in extra-microsomal Ca^{2+} levels following chlorpyrifos exposure was inhibited by approx. 50% by either DHBP, thapsigargin or heparin, suggesting its non-specific mechanism of action. The effect of chlorpyrifos on Ca^{2+} homeostasis has been reported before in the literature. For example, Meijer et al. (2014) showed increased basal Ca^{2+} levels and inhibition of depolarization-evoked Ca^{2+} influx in PC12 cells after exposure to chlorpyrifos and other organophosphates. Although, the observed inhibition of Ca^{2+} influx was mediated *via* chlorpyrifos action on VGCCs, our study suggests that the increase in basal Ca^{2+} may additionally be mediated by intracellular Ca^{2+} stores.

Notably, chloranthraniliprole and flubendiamide, potent RyR specific diamide insecticides, did not show any effect on Ca^{2+} release in rat cortical microsomes (Table 1), supporting the evidence of low mammalian toxicity and low homology between ryanodine receptors expressed in vertebrates and invertebrates (Qi and Casida, 2013).

In the present study, endosulfan and TOCP showed a significant increase in extra-microsomal Ca^{2+} levels, but their specific mechanism of action could not be clarified by inhibitor experiments. It is possible that the increase in Ca^{2+} release from microsomes exposed to endosulfan and TOCP may be attributed to increased membrane permeability as a result of oxidative stress (Rosa et al., 1996; Lakroun et al., 2015; Zhang et al., 2007). However, other potential mechanism cannot be excluded. For example, it is highly likely that next to the RyRs, IP_3Rs and SERCA, microsomal vesicles may contain other functional elements that could contribute, at least to some extent, to the observed effects mediated by the test compounds. Especially so, when the increase in Ca^{2+} release could not be explained by the co-exposure with highly specific blockers of Ca^{2+} channels and pump. It has been demonstrated that some ER membrane protein translocators, such as presenilins or SEC61-complex, can also function as Ca^{2+} leak channels (Lang et al., 2011; Tu et al., 2006; Zhang et al., 2010). These leak channels have been shown to be responsible for passive Ca^{2+} leak from the ER lumen to the cytosol, controlling the basal Ca^{2+} levels and preventing ER Ca^{2+} overload (Supnet and Bezprozvanny, 2011). Zhang et al. (2010) argued that "the enhanced ER Ca^{2+} release *via* IP_3Rs and RyRs (…) can be accounted for by the loss of ER Ca^{2+} leak function of presenilins and overloaded ER Ca^{2+} stores". It thus cannot be excluded that also in the present study compounds that showed non-specific increase in extra-microsomal Ca^{2+} levels, could act on the Ca^{2+} leak channels, or other not yet elucidated mechanisms. This is however largely speculative and further studies may clarify the exact mechanism(s) of action.

4.2. Microsomal Ca^{2+} release and uptake at different stages of brain development

In mammalian tissue, SERCA, RyR and IP_3R are expressed in three known isoforms with diverse structure and different sensitivities to pharmacological agents (Racay et al., 1996). During brain development the expression of the different isoforms undergoes dynamic changes within neurons resulting in structural and functional differentiation (Mori et al., 2000). The distribution of the isoforms differs between specific brain regions, cell types and sub cellular localizations, suggesting that distinct expression of RyR, IP_3R and SERCA isoforms may produce specific patterns of Ca^{2+} signaling (Giannini et al., 1995; Rossi et al., 2002).

Experiments using microsomes from different stages of brain development showed that microsomes from three months old (R3) female rats had more than twofold higher basal Ca^{2+} uptake activity than microsomes from adult (R6) and neonatal (RN) rats. These differences in Ca^{2+} uptake rates could not be attributed to differences in protein concentration (since each microsomal batch had been tested at the same protein concentration, 0.333 mg/ml). However, dynamic differences in expression of SERCA isoforms during brain maturation, differences in Ca^{2+} affinity between different SERCA isoforms and decline in SERCA function with advancing age (*e.g.* Baba-Aissa et al., 1998; Lytton et al., 1992; Pottorf et al., 2001) may explain, at least partially, the distinctive Ca^{2+} uptake rates observed in RN, R3 and R6 microsomes.

Interestingly, PFOS and 6-OH-BDE-47 did not show any alteration of Ca^{2+} release in RN microsomes while they showed significant effects in R3 and R6 microsomes. Several studies have suggested that not only SERCA but also RyR and IP_3R are under strict developmental control *i.e.* different isoforms are down- and up-regulated at different periods of brain development (*e.g.* Faure et al., 2001; Mori et al., 2000). Possibly, PFOS and 6-OH-BDE-47 inhibit specific isoforms of RyR and IP_3R widely expressed in adult rat brain, but not in neonatal neuronal cells.

4.3. Discussion of the methods

For many neurotoxic compounds, the cellular mechanism of action is still poorly understood. Traditional *in vivo* tests to investigate neurodevelopmental effects of environmental pollutants provide important information on behavior, motor activity and/or sensory reactivity following exposure to a test compound, but are often laborious, expensive and lack information on the specific mechanisms of toxicity at the cellular and molecular level. With the growing number of suspected (developmental) neurotoxic compounds, there is an increasing interest in the development of simplified, fast, and effective *in vitro* screening tools (Coecke et al., 2006). This study aimed at developing such a higher throughput, sensitive and robust screening method that could be used to indicate possible Ca^{2+} disrupting mechanisms of neurotoxicity and prioritize chemical for further investigation.

in vitro test systems using microsomal vesicles directly measure possible disruption of intracellular Ca^{2+} levels mediated by RyR, IP_3Rs and/or SERCA, and thus indicate potential important intracellular mechanisms of neurotoxicity. It is important to note that use of microsomal fractions does not account for other Ca^{2+} permeable channels present in the neuronal plasma membrane (*e.g.* VGCCs) that RyRs and IP_3Rs can interact with to varying degrees. However, considering that intracellular channels and pumps play a vital role in regulating intracellular Ca^{2+} homeostasis, scientific evidence suggests that interference with these processes alone can play a substantial role in the biological activity of neurotoxic compounds, including the effects observed on cellular, tissue and organism level (Bodalia et al., 2013; Chen et al., 2017; Gilbert, 2000; Howard et al., 2003; Pessah et al., 2010; Wang et al., 2015). Many suspected neurotoxic compounds, including

some compounds tested in this study, have high lipid solubility or/and high structural analogy to known neurotoxins and therefore are most likely to pass the blood-brain barrier (BBB) and reach the neuronal Ca^{2+} stores.

Results from cuvette and microplate methods were comparable and the findings for the reference compounds matched those present in the literature, suggesting that the downscaled microplate method developed for the purpose of this study could be used as a screening tool. While a single cuvette measurement takes 40 min, in the same period 40 simultaneous measurements can be made in the new downscaled microplate method. Besides being fast and cost-effective, microplate reader measurements require 10 times lower amount of microsomes than experiments in the cuvette method which saves a significant amount of biological material (and thus laboratory animals). On the other hand, the Ca^{2+} loading phase cannot be followed in real time in the microplate method. Also, quenching of the signal due to *e.g.* inhibitor addition cannot be observed, but has to be determined in advance in separate experiments.

The microplate reader method seems to be more sensitive than the cuvette method. Remarkably, all four pyrethroids tested showed an increase in Ca^{2+} release in the downscaled microplate method (Table 1), while no effect was observed for these compounds using the cuvette method (Fig. 2). Therefore, an additional experiment with alpha-cypermethrin (a representative of the pyrethroids) was performed in order to investigate the discrepancy between the two methods (see Supporting Information, Fig. S2). Our data suggest that alpha-cypermethrin binds to the microsomes in the microplate with higher affinity than in the cuvette. Although the exact mechanism underlying the discrepancy is difficult to elucidate, the increased interaction between compounds and microsomes in the microplate could provide an explanation for the observed higher sensitivity of the microplate method, at least for the pyrethroid compounds.

Despite the negative correlation between Ca^{2+} release rates and Ca^{2+} uptake rates (Section 3.3; Fig S1), effects on Ca^{2+} uptake were much less pronounced than the effects on the Ca^{2+} release induced by the same compounds. Possibly, the integrity of the microsomal membranes and/or the ATP regenerating system deteriorated by the end of the incubation period (40 min; 37 °C) when Ca^{2+} uptake was determined (Fig. 1A; slope 3). This is also suggested by the time-dependent decrease in Ca^{2+} uptake observed for the DMSO control incubation (*i.e.* slope 1 > slope 2 > slope 3). The differences in slopes may also be attributed to the fact that the concentration gradient between inter-microsomal Ca^{2+} store and extra-microsomal Ca^{2+} concentration increased with each additional Ca^{2+} spike. Consequently, Ca^{2+} storage of each new spike demanded more energy than the previous spike. Nevertheless, the results of the present study indicate that compounds that open RyR and IP_3R Ca^{2+} channels also contribute to a net decrease in Ca^{2+} uptake, whereas compounds that inhibit SERCA also contribute to a net increase in Ca^{2+} release.

Altogether, the current study shows the potential of the downscaled method to screen test compounds for their capacity to interfere with Ca^{2+} homeostasis in cerebral cortex endoplasmic reticulum with increased throughput. Our data obtained with this novel screening method indicated that representative compounds from many different chemical classes may cause increased Ca^{2+} release, and, that for some compounds this effect might be mediated through activation of RyR or IP_3R Ca^{2+} channels or inhibition of the SERCA pump (or a combination thereof). Also, our data indicated SERCA inhibition as a potential novel mechanism of action for pyrethroid insecticides. Moreover, microsomes obtained from different stages of brain maturation showed differences in sensitivity highlighting the potential of this screening method to further our understanding of the underlying age-specific mechanism of neurotoxicity. Overall, the downscaled method presented here provides a sensitive, robust, fast and informative assay that can be used to indicate potential important molecular mechanisms of neurotoxicity that should be regarded as a trigger for hypothesis building and as a tool to prioritize compounds for further investigation.

Conflict of interest

The authors declare that there are no conflicts of interest. Given his role as Editor in Chief of NeuroToxicology, Remco H.S. Westerink had no involvement in the peer-review of this article and has no access to information regarding its peer-review. Full responsibility for the editorial process for this article was delegated to Pamela J. Lein.

Acknowledgements

This study was performed within the EU FP7 funded project DENAMIC (DEvelopmental Neurotoxicity Assessment of MIxtures in Children; Contract No. 282957). The authors gratefully acknowledge Vesna Lavtizar (University of Nova Gorica, Slovenia) for providing transformation products TP1 and TP2 of chlorantraniliprole, and Sicco Brandsma and Freek Ariese (Vrije Universiteit Amsterdam) for performing the alpha-cypermethrin analyses and for hosting the fluorescence measurements on the Cary Eclipse Fluorescence Spectrophotometer, respectively. Post-mortem cortex tissue was obtained from Wistar rats sacrificed for other research projects of Vrije Universiteit Amsterdam in accordance with the European Council Directive (86/609/EEC) by permission of the Animal Research Law of The Netherlands.

Appendix A. Supplementary data

Supplementary material related to this article can be found, in the online version, at doi:https://doi.org/10.1016/j.neuro.2018.07.015.

References

Baba-Aissa, F., Raeymaekers, L., Wuytack, F., Dode, L., Casteels, R., 1998. Distribution and isoform diversity of the organellar Ca2+ pumps in the brain. Mol. Chem. Neuropathol. 33, 199–208.
Berridge, M.J., Lipp, P., Bootman, M.D., 2000. The versatility and universality of calcium signalling. Nat. Rev. Mol. Cell Biol. 1, 11–21.
Bodalia, A., Li, H., Jackson, M.F., 2013. Loss of endoplasmic reticulum Ca2+ homeostasis: contribution to neuronal cell death during cerebral ischemia. Acta Pharmacol. Sin. 34, 49–59.
Cao, Z., Shafer, T.J., Murray, T.F., 2011. Mechanisms of pyrethroid insecticide-induced stimulation of calcium influx in neocortical neurons. J. Pharmacol. Exp. Ther. 336, 197–205.
Chen, H., Streifel, K.M., Singh, V., Yang, D., Mangini, L., Wulff, H., Lein, P.J., 2017. From the cover: BDE-47 and BDE-49 inhibit axonal growth in primary rat hippocampal neuron-glia co-cultures via ryanodine receptor-dependent mechanisms. Toxicol. Sci. 156, 375–386.
Coburn, C.G., Currás-Collazo, M.C., Kodavanti, P.R.S., 2008. In vitro effects of environmentally relevant polybrominated diphenyl ether (PBDE) congeners on calcium buffering mechanisms in rat brain. Neurochem. Res. 33, 355–364.
Coecke, S., Eskes, C., Gartlon, J., Kinsner, A., Price, A., Van Vliet, E., Prieto, P., Boveri, M., Bremer, S., Adler, S., Pellizzer, C., Wendel, A., Hartung, T., 2006. The value of alternative testing for neurotoxicity in the context of regulatory needs. Environ. Toxicol. Pharmacol. 21, 153–167.
Darras, V.M., 2008. Endocrine disrupting polyhalogenated organic pollutants interfere with thyroid hormone signalling in the developing brain. The Cerebellum 7, 26–37.
Faure, A.V., Grunwald, D., Moutin, M.J., Hilly, M., Mauger, J.P., Marty, I., De Waard, M., Villaz, M., Albrieux, M., 2001. Developmental expression of the calcium release channels during early neurogenesis of the mouse cerebral cortex. Eur. J. Neurosci. 14, 1613–1622.
Gassmann, K., Schreiber, T., Dingemans, M.M.L., Krause, G., Roderigo, C., Giersiefer, S., Schuwald, J., Moors, M., Unfried, K., Bergman, Å., Westerink, R.H.S., Rose, C.R., Fritsche, E., 2014. BDE-47 and 6-OH-BDE-47 modulate calcium homeostasis in primary fetal human neural progenitor cells via ryanodine receptor-independent mechanisms. Arch. Toxicol. (88), 1537–1548.
Giannini, G., Conti, A., Mammarella, S., Scrobogna, M., Sorrentino, V., 1995. The ryanodine receptor/calcium channel genes are widely and differentially expressed in murine brain and peripheral tissues. J. Cell Biol. 128, 893–904.
Gilbert, M.E., 2000. In vitro systems as simulations of in vivo conditions: the study of cognition and synaptic plasticity in neurotoxicology. Ann. N. Y. Acad. Sci. 919, 119–132.
Gleichmann, M., Mattson, M.P., 2011. Neuronal calcium homeostasis and dysregulation. Antioxid. Redox Signal. 14, 1261–1273.
Grandjean, P., Landrigan, P., 2006. Developmental neurotoxicity of industrial chemicals.

Lancet 368, 2167–2178.
Grandjean, P., Landrigan, P.J., 2014. Neurobehavioural effects of developmental toxicity. Lancet Neurol. 13, 330–338.
Herbstman, J.B., Sjödin, A., Kurzon, M., Lederman, S.A., Jones, R.S., Rauh, V., Needham, L.L., Tang, D., Niedzwiecki, M., Wang, R.Y., Perera, F., 2010. Prenatal exposure to PBDEs and neurodevelopment. Environ. Health Perspect. 118, 712–719.
Heusinkveld, H.J., Westerink, R.H.S., 2011. Caveats and limitations of plate reader-based high-throughput kinetic measurements of intracellular calcium levels. Toxicol. Appl. Pharmacol. 255, 1–8.
Hildebrand, M.E., McRory, J.E., Snutch, T.P., Stea, A., 2004. Mammalian voltage-gated calcium channels are potently blocked by the pyrethroid insecticide allethrin. J. Pharmacol. Exp. Ther. 308, 805–813.
Howard, A.S., Fitzpatrick, R., Pessah, I., Kostyniak, P., Lein, P.J., 2003. Polychlorinated biphenyls induce caspase-dependent cell death in cultured embryonic rat hippocampal but not cortical neurons via activation of the ryanodine receptor. Toxicol. Appl. Pharmacol. 190, 72–86.
Hu, H., Téllez-Rojo, M.M., Bellinger, D., Smith, D., Ettinger, A.S., Lamadrid-Figueroa, H., Schwartz, J., Schnaas, L., Mercado-García, A., Hernández-Avila, M., 2006. Fetal lead exposure at each stage of pregnancy as a predictor of infant mental development. Environ. Health Perspect. 114, 1730–1735.
Jolous-Jamshidi, B., Cromwell, H.C., McFarland, A.M., Meserve, L.A., 2010. Perinatal exposure to polychlorinated biphenyls alters social behaviors in rats. Toxicol. Lett. 199, 136–143.
Kenet, T., Froemke, R.C., Schreiner, C.E., Pessah, I.N., Merzenich, M.M., 2007. Perinatal exposure to a noncoplanar polychlorinated biphenyl alters tonotopy, receptive fields, and plasticity in rat primary auditory cortex. Proc. Natl. Acad. Sci. U. S. A. 104, 7646–7651.
Kim, K.H., Pessah, I.N., 2011. Perinatal exposure to environmental polychlorinated biphenyls sensitizes hippocampus to excitotoxicity ex vivo. Neurotoxicology 32, 981–985.
Kim, K.H., Bose, D.D., Ghogha, A., Riehl, J., Zhang, R., Barnhart, C.D., Lein, P.J., Pessah, I.N., 2011. Para- and ortho-substitutions are key determinants of polybrominated diphenyl ether activity toward ryanodine receptors and neurotoxicity. Environ. Health Perspect. 119, 519–526.
Kodavanti, P.R.S., Ward, T.R., 2005. Differential effects of commercial polybrominated diphenyl ether and polychlorinated biphenyl mixtures on intracellular signaling in rat brain in vitro. Toxicol. Sci. 85, 952–962.
Lakroun, Z., Kebieche, M., Lahouel, A., Zama, D., Desor, F., Soulimani, R., 2015. Oxidative stress and brain mitochondria swelling induced by endosulfan and protective role of quercetin in rat. Environ. Sci. Pollut. Res. Int. 22, 7776–7781.
Lang, S., Erdmann, F., Jung, M., Wagner, R., Cavalié, A., Zimmermann, R., 2011. Sec61 complexes form ubiquitous ER Ca^{2+} leak channels. Channels 5, 228–235.
Langeveld, W.T., Meijer, M., Westerink, R.H.S., 2012. Differential effects of 20 non-dioxin-like PCBs on basal and depolarization-evoked intracellular calcium levels in PC12 cells. Toxicol. Sci. 126, 487–496.
Lavtizar, V., Van Gestel, C.A.M., Dolenc, D., Trebse, P., 2014. Chemical and photochemical degradation of chlorantraniliprole and characterization of its transformation products. Chemosphere 95, 408–414.
Liu, X., Jin, Y., Liu, W., Wang, F., Hao, S., 2011. Possible mechanism of perfluorooctane sulfonate and perfluorooctanoate on the release of calcium ion from calcium stores in primary cultures of rat hippocampal neurons. Toxicol. In Vitro 25, 1294–1301.
Llansola, M., Montoliu, C., Boix, J., Felipo, V., 2010. Polychlorinated biphenyls PCB 52, PCB 180, and PCB 138 impair the glutamate-nitric oxide-cGMP pathway in cerebellar neurons in culture by different mechanisms. Chem. Res. Toxicol. 23, 813–820.
Lyall, K., Croen, L.A., Sjödin, A., Yoshida, C.K., Zerbo, O., Kharrazi, M., Windham, G.C., 2017. Polychlorinated biphenyl and organochlorine pesticide concentrations in maternal mid-pregnancy serum samples: association with Autism spectrum disorder and intellectual disability. Environ. Health Perspect. 125, 474–480.
Lytton, J., Westlin, M., Burk, S.E., Shull, G.E., MacLennan, D.H., 1992. Functional comparisons between isoforms of the sarcoplasmic or endoplasmic reticulum family of calcium pumps. J. Biol. Chem. 267, 14483–14489.
Marambaud, P., Dreses-Werringloer, U., Vingtdeux, V., 2009. Calcium signaling in neurodegeneration. Mol. Neurodegener. 4, 20.
Meijer, M., Dingemans, M.M.L., van den Berg, M., Westerink, R.H.S., 2014. Inhibition of voltage-gated calcium channels as common mode of action for (mixtures of) distinct classes of insecticides. Toxicol. Sci. 141, 103–111.
Michelangeli, F., East, J.M., 2011. A diversity of SERCA Ca2+ pump inhibitors. Biochem. Soc. Trans. 39, 789–797.
Mori, F., Fukaya, M., Abe, H., Wakabayashi, K., Watanabe, M., 2000. Developmental changes in expression of the three ryanodine receptor mRNAs in the mouse brain. Neurosci. Lett. 285, 57–60.
Myers, G.J., Davidson, P.W., 1998. Prenatal methylmercury exposure and children: neurologic, developmental, and behavioral research. Environ. Health Perspect. 106 (Suppl 3), 841–847.
Nakamura, R., Teshima, R., Sawada, J., ichi, 2002. Effect of dialkyl phthalates on the degranulation and Ca2+ response of RBL-2H3 mast cells. Immunol. Lett. 80, 119–124.
Paterson, S.J., Heim, S., Friedman, J.T., Choudhury, N., Benasich, A.A., 2006. Development of structure and function in the infant brain: implications for cognition, language and social behaviour. Neurosci. Biobehav. Rev. 30, 1087–1105.
Pessah, I.N., Hansen, L.G., Albertson, T.E., Garner, C.E., Ta, T.A., Do, Z., Kim, K.H., Wong, P.W., 2006. Structure-activity relationship for noncoplanar polychlorinated biphenyl congeners toward the ryanodine receptor-Ca2+ channel complex type 1 (RyR1). Chem. Res. Toxicol. 19, 92–101.
Pessah, I.N., Cherednichenko, G., Lein, P.J., 2010. Minding the calcium store: ryanodine receptor activation as a convergent mechanism of PCB toxicity. Pharmacol. Ther. 125, 260–285.
Pottorf, W.J., De Leon, D.D., Hessinger, D.A., Buchholz, J.N., 2001. Function of SERCA mediated calcium uptake and expression of SERCA3 in cerebral cortex from young and old rats. Brain Res. 914, 57–65.
Qi, S., Casida, J.E., 2013. Species differences in chlorantraniliprole and flubendiamide insecticide binding sites in the ryanodine receptor. Pestic. Biochem. Physiol. 107, 321–326.
Racay, P., Kaplán, P., Lehotský, J., 1996. Control of Ca2+ homeostasis in neuronal cells. Gen. Physiol. Biophys. 15, 193–210.
Rauh, V.A., Garfinkel, R., Perera, F.P., Andrews, H.F., Hoepner, L., Barr, D.B., Whitehead, R., Tang, D., Whyatt, R.W., 2006. Impact of prenatal chlorpyrifos exposure on neurodevelopment in the first 3 years of life among inner-city children. Pediatrics 118, e1845–1859.
Rauh, V., Arunajadai, S., Horton, M., Perera, F., Hoepner, L., Barr, D.B., Whyatt, R., 2011. Seven-year neurodevelopmental scores and prenatal exposure to chlorpyrifos, a common agricultural pesticide. Environ. Health Perspect. 119, 1196–1201.
Rengifo, J., Gibson, C.J., Winkler, E., Collin, T., Ehrlich, B.E., 2007. Regulation of the inositol 1,4,5-trisphosphate receptor type I by O-GlcNAc glycosylation. J. Neurosci. 27, 13813–13821.
Rice, D., Barone, S., 2000. Critical periods of vulnerability for the developing nervous system: evidence from humans and animal models. Environ. Health Perspect. 108 (Suppl 3), 511–533.
Rizzuto, R., 2001. Intracellular Ca(2+) pools in neuronal signalling. Curr. Opin. Neurobiol. 11, 306–311.
Rosa, R., Rodriguez-Farré, E., Sanfeliu, C., 1996. Cytotoxicity of hexachlorocyclohexane isomers and cyclodienes in primary cultures of cerebellar granule cells. J. Pharmacol. Exp. Ther. 278, 163–169.
Rossi, D., Simeoni, I., Micheli, M., Bootman, M., Lipp, P., Allen, P.D., Sorrentino, V., 2002. RyR1 and RyR3 isoforms provide distinct intracellular Ca2+ signals in HEK 293 cells. J. Cell. Sci. 115, 2497–2504.
Roze, E., Meijer, L., Bakker, A., Van Braeckel, K.N.J.A., Sauer, P.J.J., Bos, A.F., 2009. Prenatal exposure to organohalogens, including brominated flame retardants, influences motor, cognitive, and behavioral performance at school age. Environ. Health Perspect. 117, 1953–1958.
Soderlund, D.M., 2012. Molecular mechanisms of pyrethroid insecticide neurotoxicity: recent advances. Arch. Toxicol. 86, 165–181. https://doi.org/10.1007/s00204-011-0726-x.
Supnet, C., Bezprozvanny, I., 2011. Presenilins function in ER calcium leak and Alzheimer's disease pathogenesis. Cell Calcium 50, 303–309.
Tan, Y., Song, R., Lawrence, D., Carpenter, D.O., 2004. Ortho-substituted but not coplanar PCBs rapidly kill cerebellar granule cells. Toxicol. Sci. 79, 147–156.
Testa, C., Nuti, F., Hayek, J., De Felice, C., Chelli, M., Rovero, P., Latini, G., Papini, A.M., 2012. Di-(2-Ethylhexyl) phthalate and autism spectrum disorders. ASN Neuro 4, 223–229.
Tu, H., Nelson, O., Bezprozvanny, A., Wang, Z., Lee, S.F., Hao, Y.H., Serneels, L., De Strooper, B., Yu, G., Bezprozvanny, I., 2006. Presenilins Form ER Ca2+ leak channels, a function disrupted by familial Alzheimer's disease-linked mutations. Cell 126, 981–993.
Tully, K., Kupfer, D., Dopico, A.M., Treistman, S.N., 2000. A plasticizer released from IV drip chambers elevates calcium levels in neurosecretory terminals. Toxicol. Appl. Pharmacol. 168, 183–188.
Verkhratsky, A., Parpura, V., 2014. Calcium signalling and calcium channels: evolution and general principles. Eur. J. Pharmacol. 739, 1–3.
Wang, Y., Zhao, H., Zhang, Q., Liu, W., Quan, X., 2015. Perfluorooctane sulfonate induces apoptosis of hippocampal neurons in rat offspring associated with calcium overload. Toxicol. Res. (Camb). 4, 931–938.
Wayman, G.A., Bose, D.D., Yang, D., Lesiak, A., Bruun, D., Impey, S., Ledoux, V., Pessah, I.N., Lein, P.J., 2012. PCB-95 modulates the calcium-dependent signaling pathway responsible for activity-dependent dendritic growth. Environ. Health Perspect. 120, 1003–1009.
Westerink, R.H.S., 2014. Modulation of cell viability, oxidative stress, calcium homeostasis, and voltage- and ligand-gated ion channels as common mechanisms of action of (mixtures of) non-dioxin-like polychlorinated biphenyls and polybrominated diphenyl ethers. Environ. Sci. Pollut. Res. Int. 21, 6373–6383.
Wong, P.W., Pessah, I.N., 1996. Ortho-substituted polychlorinated biphenyls alter calcium regulation by a ryanodine receptor-mediated mechanism: structural specificity toward skeletal- and cardiac-type microsomal calcium release channels. Mol. Pharmacol. 49, 740–751.
Wong, P.W., Brackney, W.R., Pessah, I.N., 1997. Ortho-substituted polychlorinated biphenyls alter microsomal calcium transport by direct interaction with ryanodine receptors of mammalian brain. J. Biol. Chem. 272, 15145–15153.
Wong, P.W., Garcia, E.F., Pessah, I.N., 2001. ortho-substituted PCB95 alters intracellular calcium signaling and causes cellular acidification in PC12 cells by an immunophilin-dependent mechanism. J. Neurochem. 76, 450–463.
Zhang, H., Sun, S., Herreman, A., De Strooper, B., Bezprozvanny, I., 2010. Role of Presenilins in Neuronal Calcium Homeostasis. J. Neurosci. 30, 8566–8580.
Zhang, L.P., Wang, Q.S., Zhu, J., Zhou, G.Z., Xie, K.Q., 2007. Time-dependent changes of lipid peroxidation and antioxidative status in nerve tissues of hens treated with tri-ortho-cresyl phosphate (TOCP). Toxicology 239, 45–52.
Zimányi, I., Pessah, I.N., 1991. Comparison of [3H]ryanodine receptors and Ca++ release from rat cardiac and rabbit skeletal muscle sarcoplasmic reticulum. J. Pharmacol. Exp. Ther. 256, 938–946.